



Contents lists available at ScienceDirect

# Computer Methods and Programs in Biomedicine

journal homepage: [www.elsevier.com/locate/cmpb](http://www.elsevier.com/locate/cmpb)

## The contribution of upper and lower body arterial vessels to the aortic root reflections: A one-dimensional computational study

Shima Abdullateef<sup>a,b</sup>, Ashraf W. Khir<sup>c,\*</sup><sup>a</sup> Centre for Medical Informatics, Usher Institute, College of Medicine and Veterinary Medicine, University of Edinburgh, Edinburgh, United Kingdom<sup>b</sup> Department of Mechanical and Aerospace Engineering, Brunel University London, Uxbridge, United Kingdom<sup>c</sup> Bioengineering Group, Department of Engineering, Durham University, Durham, United Kingdom

### ARTICLE INFO

#### Article history:

Received 25 January 2023

Revised 12 May 2023

Accepted 12 May 2023

#### Keywords:

Reflected wave

Reflection site

Reflection coefficient

Wave speed

Transmission coefficient

Wave intensity

1D computational model

### ABSTRACT

**Background and Objectives:** Reflections measured at the aortic root are of physiological and clinical interest and thought to be composed of the superimposed reflections arriving from the upper and lower parts of the circulatory system. However, the specific contribution of each region to the overall reflection measurement has not been thoroughly examined. This study aims to elucidate the relative contribution of reflected waves arising from the upper and lower human body vasculature to those observed at the aortic root.

**Methods:** We utilised a one-dimensional (1D) computational model of wave propagation to study reflections in an arterial model that included 37 largest arteries. A narrow Gaussian-shaped pulse was introduced to the arterial model from five distal locations: carotid, brachial, radial, renal, and anterior tibial. The propagation of each pulse towards the ascending aorta was computationally tracked. We calculated the reflected pressure and wave intensity at the ascending aorta in each case. The results are presented as a ratio of the initial pulse.

**Results:** The findings of this study indicates that pressure pulses originated at the lower body can hardly be observed, while those originated from the upper body account for the largest portion of reflected waves seen at the ascending aorta.

**Conclusions:** Our study validates the findings of earlier studies, which demonstrated that human arterial bifurcations have a significantly lower reflection coefficient in the forward direction as compared to the backward direction. The results of this study underscore the need for further *in-vivo* investigations to provide a deeper understanding of the nature and characteristics of reflections observed in the ascending aorta, which can inform the development of effective strategies for the management of arterial diseases.

© 2023 The Authors. Published by Elsevier B.V.

This is an open access article under the CC BY-NC-ND license (<http://creativecommons.org/licenses/by-nc-nd/4.0/>)

### 1. Introduction

Arterial wave reflections and their influence on the contour of the pressure waveform in the aorta has been widely studied [1–5]. With each cardiac cycle, a wave propagates forward towards the periphery, while alterations in the arterial mechanical and geometrical properties, such as elastic modulus, dimensions, and morphology can cause reflections that travel backward towards the heart. From a theoretical standpoint, optimal wave transmission and minimal wave reflection is attained when the ratio of wall thickness to vessel radius remains constant before and after the junction (i.e., optimal area ratio). Notably, Papageorgiou and col-

leagues [6] studied 444 junctions at various locations in the human arterial tree and concluded that the area ratio of the daughter to the parent vessel for forward-travelling waves was approximately 1.14, consistent with the theoretical optimal area ratio, except for the aortoiliac bifurcation where a lower value was observed. In this context, we note that bifurcations with an optimal area ratio for forward travelling waves (i.e., travelling from the parent vessels to the daughter vessels) constitutes a strong reflection site for backward travelling waves (i.e., travelling from a daughter vessel to the parent and the other daughter vessel). Consequently, backward travelling waves are significantly damped as they travel back towards the heart. Furthermore, any backward-travelling reflected wave can undergo re-reflection and travel in the forward direction until encountering another discontinuity and reflecting again, a phenomenon known as wave-trapping. The complexity of wave trapping suggests that keeping track of the reflections traversing the arterial system is not trivial [7–10].

\* Corresponding author at: Department of Engineering, Durham University, South Rd., Durham, DH1 3LE.

E-mail address: [ashraf.w.khir@durham.ac.uk](mailto:ashraf.w.khir@durham.ac.uk) (A.W. Khir).

Several studies have focused on understanding wave reflections and identifying the principal reflection sites along the arterial tree [3,5,11,12]. In a classical experiment, Peterson and Gerst [13] injected controlled volume pulses at peripheral arterial locations in living dogs and found no evidence of the injected waves reaching the aortic root. This led them to conclude that reflected waves might not affect the central arterial pulse contour, as they are progressively damped by the arterial tree. In another experimental study, Khir and Parker [12] occluded the aorta of dogs at four different locations and reported that reflection in the aortic root due to the occlusion was similar to the control condition (i.e. no occlusion) when the occlusion site was below the renal bifurcations.

Different *in-vitro* models of the circulation were introduced to investigate arterial wave transmission, mainly consisting of single tube [14,15] and T-tube models [16,17]. The single tube model is primarily used to study the interaction between the heart and the arterial tree with a single reflection site. On the other hand, T-tube models are used with the assumption of the existence of two separate reflection sites. Burattini and Campbell [16] used a modified T-tube model and questioned the concept of the existence of a discrete reflection site, concluding that the middle to low abdominal aorta is the “effective reflection site”.

More recently, *in-vitro* models were extended to detailed arterial replicas. Segers and Verdonck [18] used an elastic replica of large conduit arteries to study the pattern of reflected waves in the aorta and compared the *in-vitro* results with those estimated by computational models. After the separating the pressure waveform into its incident and reflected components, they observed continuous reflections originating at different locations of the replica. They extrapolated that the reflected waveforms observed in aortic *in-vivo* are an interaction between small reflections arising from tapering and those originating at the diaphragm level.

Arterial wave reflections have been investigated also *in-vivo*, with Murgo et al. [19] and Mills et al. [20] reporting that reflections originating from the end of the abdominal aorta are the main contributor to reflections observed in the ascending aorta. A secondary outcome of the study of Murgo et al. [19] is that bilateral external compression of the femoral arteries resulted in increased pressure at ascending aorta in four patients, thus suggesting that partial occlusions of peripheral arteries may enhance reflections in the aorta. These findings were corroborated by Murakami [21], who observed an increase aortic pressure during squatting, which compresses the femoral arteries. Furthermore, Latham et al. [22] identified two major sites of arterial wave reflection that impact the aortic pressure, namely the renal branches and the aorta-iliac bifurcation.

Numerous *in-vivo* studies investigated the effect of aging and pathologies on wave reflections [4,23–25]. Segers et al. [26] showed that the magnitude of wave reflections increases with age, and Greenwald et al. [27] reported that the area ratio of parent to daughters vessels at the aorta-iliac bifurcation changes with age, from +0.3 in early life to –0.3 in old age, indicating the potential change of the nature of the wave reflection from compression to expansion. Furthermore, several studies have explored the changes in wave reflections associated with abdominal aortic aneurysm, aortic coarctation and arterial stenosis [28–31].

Despite these findings, there is debate among researchers regarding the significance of reflected waves from peripheral vessels in the ascending aorta [12,13]. While some studies have observed a measurable change in the arterial pressure due to semi-occlusion in femoral arteries [21], others have suggested that reflections arise from multiple sites rather than a single location [3,11]. To our knowledge, no published works have explored the relative contribution of reflections originating from upper and lower body vessels to the pressure observed in ascending aorta. Thus, the ques-

tion about the composition of aortic root reflections remains open for further investigation.

As a contribution to the above open question regarding the origin of reflections in the ascending aorta, we propose that peripherally originated reflections lose much of their amplitude before reaching the aortic root. To test this hypothesis, we utilised a one-dimensional (1D) computational model developed by Matthys et al. [32], which has demonstrated the ability to capture the main features of human conduit artery pressure and flow waveforms. By initiating a pulse from distal sites and tracking changes in pressure and wave intensity, we assessed the pulse's transmission to the aortic root. Additionally, we compared reflection coefficient as the pulse encounters the bifurcation in the forward and backward directions and investigated the relative contribution of upper and lower body vessel reflections to the pressure in the ascending aorta.

## 2. Methods

### 2.1. Numerical model

The one-dimensional model of pulse wave propagation used in this study is based on the physical principles of conservation of mass and momentum and on the tube-law, under the assumption that blood is incompressible and Newtonian, the flow is laminar, and that there are no energy losses at bifurcations [33]. The conservation equations and tube-law are numerically solved using a discontinuous Galerkin scheme with a spectral/hp spatial discretization. The connections at the interface of the arterial segments are governed by the conservation of mass and continuity of total pressure.

An arterial network composed of the 37 largest arteries is modelled to study the proportion of a reflected wave travelling towards the aorta from distal locations. This numerical model is designed and validated by a 1:1 silicon replica of the largest arterial vessels [33]. The large vessels in this model were linearly tapered, and the smallest branches had a constant cross-sectional area. Elastic modulus value of 1.2 MPa used for the aortic wall in the current work was taken after 1D numerical model of the arterial tree [33]. The silicon wall's performance was evaluated under physiological pressure conditions, and it was found to have a consistent Young's modulus of 1.2 MPa throughout the working pressure range. This value is within the reported values of recent mechanical testing of the human aorta [34], and also found in the classical review by Dobrin [35]. Hence, the choice of elastic modulus used in this work is representative to physiological conditions and well justified.

The end branches of the system are modelled as simple resistance models with a stiff capillary tube leading to an overflow reservoir that reflects a constant venous pressure. The necessary parameters for the numerical algorithm are obtained directly from *in vitro* measurements [32]. In the numerical model, peripheral resistance to the flow is determined by measuring mean pressure and flow measurements in close proximity to the outlet of each terminal branch. These measurements are then simulated as an outflow boundary condition by implementing the equation  $R_p = (p_{1D} - p_{out})/Q_{1D}$ , where  $R_p$  denotes the peripheral resistance,  $p_{1D}$  and  $Q_{1D}$  are the pressure and flow rate at the outlet of 1D terminal branch. The constant hydrostatic pressure at the overflow reservoir is assigned a value of 3.2 mmHg and used as the value for  $p_{out}$ .

Table 1 in the reference [32] provides detailed information about the dimensions of the vessels, including the diastolic cross-sectional radii at the inlet and outlet of each segment, the average wall thickness, and the peripheral resistance values. This model produces physiologically accurate pressure and velocity waves with a physiological inflow boundary condition. Figs. 1A and 1B depict

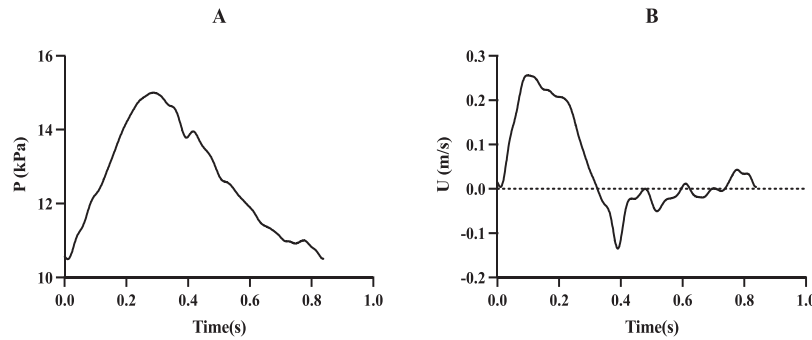


**Fig. 1.** The simulated pressure ( $P$ ) in A, and velocity ( $U$ ), in B, at the level of ascending aorta in the 37-segment numerical 1D model generated by a physiological inflow boundary condition.

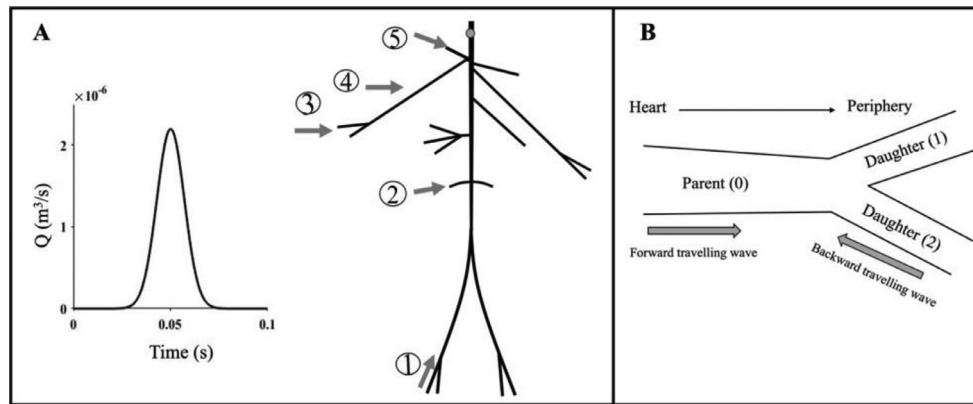


**Fig. 2.** A) A narrow Gaussian-shaped flow used as input (left) and the schematic representation of the arterial network with locations of insertion of the pulse (right). In five different simulations the pulse was inserted from 1) right anterior tibial artery, 2) the right renal artery, 3) the right radial artery, 4) the right brachial artery, and 5) the right carotid artery. B) A schematic representation of a bifurcation and the travelling waves directions.

**Table 1**

Estimated values for the transmission coefficient for backward travelling waves using three different calculation methods.

JUNCTION	$1 + R_t$	$1 + R_{dp}$	$1 + R_{dl}^{0.5}$
Tibial bifurcation	0.551	0.605	0.518
Iliac bifurcation	0.223	0.222	0.195
Abdominal aorta to renal	0.127	0.180	0.178
Abdominal aorta to celiac	0.187	0.153	0.166
Brachial bifurcation	0.598	0.606	0.519
Brachiocephalic bifurcation	0.522	0.477	0.571

the pressure and velocity waves computed by this model as the physiological inflow ( $Q$ ) is the input boundary condition.

Using a pulse as the input to the arterial model is convenient for testing the response of the system and showing both the reflections and changes in the amplitude of the pulse as it propagates through the system [9]. A narrow Gaussian-shaped flow wave, with an amplitude large enough to reach the ascending aorta, was inserted into various distal vessels. The shape of the inflow is defined as

$$Q(t) = 2.2 * 10^{-6} e^{-10,000(t-0.05)^2} \text{ (m}^3\text{s}^{-1}\text{)} \quad (1)$$

and can be seen in Fig. 2A. The terminal vessels in each simulation are connected to a single resistance in a Windkessel model unless that vessel is chosen for inducing the volume inflow. Fig. 2 indicates the selected origins for the pulses: 1) the right femoral artery, 2) the right renal artery, 3) the right radial artery, 4) the right brachial artery, and 5) the right common carotid artery. The initial conditions for all segments are  $(A(x, 0), U(x, 0), P(x, 0)) = (A_0(x), 0, 0)$ .  $A$ ,  $U$ , and  $P$  are cross-sectional area, velocity, and pressure, respectively.  $A_0$  is the initial cross-sectional area at

time=0. To isolate the changes of reflections arising from distal locations, no cardiac input was introduced into the system, and the aortic valve was considered closed, in all simulations. For the scenario where the pulse is inserted into the brachial artery (No. 4), which is not a terminal segment, the connected distal segments are excluded from the model, and a pulse inflow replaces the terminal boundary condition.

Since the same pulse was inserted into different vessels, the amplitudes of the generated pressure were different at each location. This difference is attributed to the varying cross-sectional areas of the distal vessels, which result in different flow velocities ( $Q = AU$ ). Therefore, to facilitate comparisons between different sites, the pressure values in the ascending aorta were normalised to the pressure of the pulse inserted in that location. For instance, the pressure wave arriving at the ascending aorta from the renal artery is normalised by dividing its maximum value by the peak pressure in the renal vessel.

## 2.2. Wave intensity analysis

Wave intensity analysis (WIA) determines the flux of energy carried by the wave per cross-sectional area, and it is calculated using Eq. (2)

$$dI_{f,b} = dP_{f,b} dU_{f,b} = \pm \frac{1}{4\rho c} (dP \pm \rho c dU)^2, \quad (2)$$

where  $P$  and  $U$  denote the fluid pressure and velocity, and subscripts f and b indicate the forward and backward wave components. The SI unit of WIA is  $W/m^2$ . Wave speed ( $c$ ) is obtained using the Moens-Korteweg equation [36] and fluid density  $\rho$  is set to  $1050 \text{ kg m}^{-3}$ .

Nonlinear separation of the wavefronts has previously been studied [37–39]. However, Pythoud et al. [38] showed that the difference between the linear and nonlinear results was 5–10%, with the linear separation being sufficient for practical purposes.

### 2.3. Calculation of reflection and transmission coefficient

To begin, the definition of reflection coefficient ( $R$ ) was extended from its use in acoustic waves to arterial modeling. In acoustics,  $R$  is defined as the ratio of the energy of the reflected- to the incident wave [40]. In physiological fluid mechanics,  $R$  is most often defined as the ratio of the amplitude of the reflected to the incident pressure wave, given that the unit for pressure is energy per unit volume [8]. In addition,  $R$  can be calculated using wave intensity analysis [41]. In this work, we compared three methods for estimating  $R$  in a tapered arterial network, as no previous studies have reported on different estimation methods for this application.

- (i) The first method uses the impedance ( $Z$ ) of the vessels in the bifurcation, and it is written as

$$R_t = \frac{1/Z_0 - 1/Z_1 - 1/Z_2}{1/Z_0 + 1/Z_1 + 1/Z_2}; \quad Z = \frac{\rho c}{A} \quad (3)$$

Where  $R_t$  is the theoretically calculated reflection coefficient. Subscripts 0, 1, and 2 indicate parent vessel and daughter vessels 1 and 2. It is worth mentioning that if waves encounter an increase in the impedance at a bifurcation, the reflection coefficient will be positive, and the opposite holds true. The size of the reflected wave and its nature (compression ( $dP > 0$ ) /decompression ( $dP < 0$ ); increase/decrease in pressure) is determined as the product of the incident wave and the reflection coefficient. For example, an incident compression wave encountering a negative reflection coefficient will produce a reflected decompression wave, whereas a positive reflection coefficient would result in a reflected compression wave. Similarly, an incident decompression wave encountering a negative reflection coefficient will produce a reflected compression wave, whereas encountering a positive reflection coefficient will produce a reflected decompression wave [11,42].

Assuming that blood is incompressible, Eq. (3) reduces to

$$R_{t, \text{parent}} = \frac{A_0/c_0 - A_1/c_1 - A_2/c_2}{A_0/c_0 + A_1/c_1 + A_2/c_2} \quad (4)$$

Equation (4) can also be written for a wave approaching the bifurcation from one of the daughter vessels as

$$R_{t, \text{daughter } 1} = \frac{A_1/c_1 - A_0/c_0 - A_2/c_2}{A_0/c_0 + A_1/c_1 + A_2/c_2} \quad (5)$$

This equation can be used for the theoretical calculation of the reflection coefficient, using only the structural properties of the vessel. A schematic representation of a bifurcation the direction of the wave is shown in Fig. 2B.

- (i) The second approach [43] is to use the ratio of net changes in the peak of backward pressure ( $\Delta P_b$ ) to the peak of forward pressure ( $\Delta P_f$ ) waves as

$$R_{dp} = \frac{\Delta P_b}{\Delta P_f}, \quad (6)$$

where  $\Delta P_{f,b} = \Sigma dP_{f,b}$  and  $dP_{f,b} = \frac{1}{2}(dP \pm \rho cdU)$ . In this work, references to  $R_{dp}$  are the values resulting from the simulations.

- (i) The third method [44] for estimation of  $R$  used is defined as the square root of the ratio of peak backward wave intensity ( $\Delta I_b$ ) to peak forward wave intensity ( $\Delta I_f$ ) written as

$$R_{dl}^{0.5} = \pm \sqrt{\frac{|\Delta I_b|}{\Delta I_f}} \quad (7)$$

The sign for  $R_{dl}^{0.5}$  is positive if the reflection is in the same direction of the incident wave and negative if they are different. Similar to  $R_{dp}$ ,  $R_{dl}^{0.5}$  is estimated using the values resulting from the simulations.

The transmission coefficient (i.e. the parameter quantifying the amount of wave transmitted after a bifurcation [31] is related to the reflection coefficient and calculated as

$$T = 1 + R \quad (8)$$

For estimating the reduction of the pressure wave in the simulations, as it crosses the bifurcations, the amplitude of the wave can be calculated using

$$\text{Amp}_p = P_p * \prod_{k=1}^n (1 + R_k) = P_p * \prod_{k=1}^n T_k, \quad (9)$$

where  $P_p$  is the peak pressure at the distal inlet and  $R_k$  and  $T_k$  are the reflection and transmission coefficients of the  $k^{\text{th}}$  bifurcation, respectively.

To avoid confusion with the established notions, it is important to clarify that introducing a pulse as a reflection into a system is not equivalent to a reflected wave. This is because the pulse is generated as an outcome of an incident wave encountering a reflection site. Therefore, establishing systematic definitions are necessary for this study. Any wave travelling from the distal locations towards the heart, regardless of its source, is a backward wave, and any wave travelling from the heart towards the peripheral beds is a forward travelling wave. It is important to note that reflected waves can travel in both forward and backward directions. For example, if a reflected wave reaches the closed aortic valve, it will be re-reflected in the forward direction.

### 3. Results

For each of the five scenarios of backward wave propagation, we performed numerical simulations to investigate the changes in pressure and velocity along the path leading to the ascending aorta. At each main bifurcation point between the distal site and the ascending aorta, we separated the pressure and wave intensity into their forward and backward components, as shown in Fig. 3. We then used the peak values of these separated components to calculate  $R_{dp}$  and  $R_{dl}^{0.5}$ .

The calculated transmission coefficient for the different bifurcations ( $T_{rev}$ ) is presented in Table 1. The results demonstrated in the table reveal that the iliac bifurcation and the aortic-renal and aortic-celiac junctions constitute the major sites of reflections for backward travelling waves, with approximately 80% of the pressure wave (re)reflected towards the peripheral circulations.

On the other hand, approximately 40–50% of the backward wave's amplitude is transmitted to the parent vessel at the tibial, brachial and brachiocephalic bifurcations. Fig. 4 provides an example of the propagation of a backward pressure injected from the anterior-tibial artery towards the ascending aorta. Because of wave reflections at the lower limb arterial bifurcations, only a small fraction ( $\sim 0.3$ ) of the injected wave reaches the abdominal aorta before being further damped at major aortic bifurcations sites such as the renal and celiac arteries.

Using Eqs. (4) and (5), the theoretical reflection coefficient for each major bifurcation in the model was calculated for waves entering the bifurcation in the forward (travelling away from the heart) and in the backward direction (travelling towards the heart) and presented in Table 2. The results reveal that, in most bifurcation, the reflection coefficients for forward travelling waves are smaller in absolute value than those for backward travelling waves. This indicates that, on average, waves entering a bifurcation from the parent tube in the forward direction lose far less amplitude

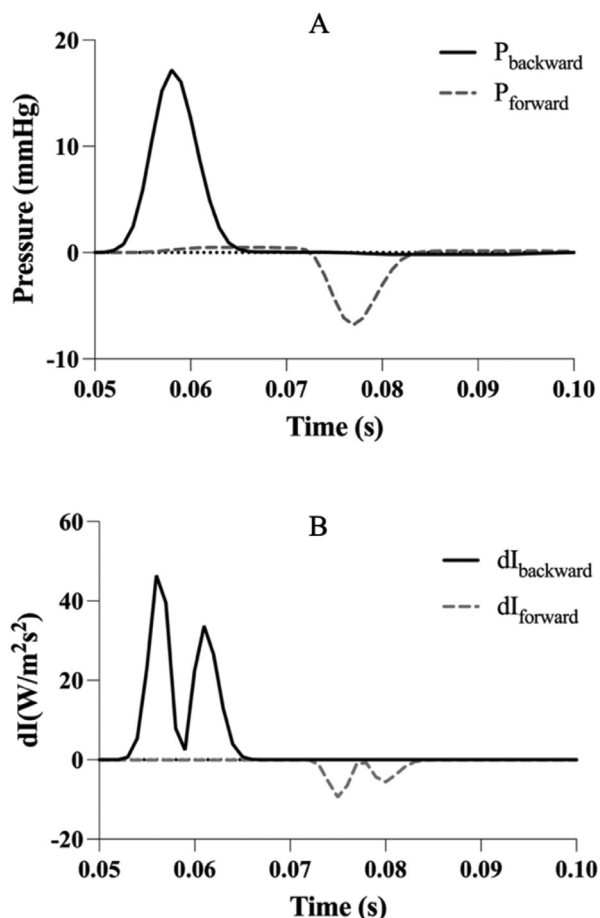


**Fig. 3.** The forward and backward components of the pressure (A) and wave intensity (B) generated by a narrow Gaussian-shaped pulse inserted at right anterior tibial artery.  $dI_{\text{backward}}$  and  $dI_{\text{forward}}$  are the intensity of the wave travelling from the periphery to the ascending aorta and vice-versa, respectively.

due to reflection than those entering from one of the daughter tubes in the backward direction.

For each of the five considered scenarios, we employed Eq. (9) and the backward travelling wave reflection coefficients from Table 2 to estimate the attenuation of the injected backward pressure wave as it propagates towards the aortic root. We then compared these estimations with the results obtained from our 1D model simulations. Fig. 5 illustrates this comparison, which has been normalised with respect to the input pressure and wave intensity values. Fig. 5 displays an exponential fitting for the decline of pressure and backward wave intensity using dashed and solid lines. Theoretical calculations and simulation results are presented by triangle and square markers, respectively.

To examine the effect of the size of the inserted pulse representing the reflected wave on the results, we repeated the computational experiments whilst doubling and tripling the amplitudes of the inserted pulses. We found that varying the amplitudes of the inserted pulses yielded similar results to those obtained with the currently used amplitude. Given that the reflection arriving at the ascending aorta is reported as a ratio of the original pulse, and since the reflection coefficient of the arterial bifurcations and the effect of tapering are independent of pulse amplitude, this finding was unsurprising.

Furthermore, the ratio between the amplitude of the pressure wave inserted at the distal location and the amplitude of the wave reaching the ascending aorta is presented in Fig. 6. As the theoretical prediction showed good agreement with values obtained from

the 1D modeling simulations, particularly for pressure amplitudes (right panels in Fig. 5). The backward pressure wave inserted in the carotid artery, due to its proximity to the heart, exhibited the highest relative amplitude at the aortic root (approaching 20% of the input), which is roughly twice as high as that observed in the brachial artery. In contrast, the other three sites showed significant damping, with more than 95% reduction in the amplitude of the injected pressure wave.

To investigate the influence of pulse width on the normalised pressure amplitudes, we repeated the simulations with pulse widths ranging from 0.01 to 0.3 s. As depicted in Fig. 7, there were no discernible changes in the normalised pressure amplitude across different widths.

#### 4. Discussions

This study aimed to better understand the composition of reflected waves measured in the ascending aorta, which is assumed to be the results of reflections from both lower and upper body. However, the contribution of each body part to the total measured reflections is not adequately understood. In this work, we used a 1D multi-branching and validated model representing the 37 largest vessels of the human arterial tree to investigate the attenuation in the amplitude of the wave travelling in the backward direction as it is generated from distal sites. We separated the waves into their forward and backward components and found that a significant proportion of the ‘reflection waves’ travelling from lower body to the ascending aorta are re-reflected towards the peripheral circulation. On the contrary, reflections originating from the upper body and, in particular, the carotid artery are less reflected on their route to the ascending aorta.

As the pulse wave generated by contracting ventricle travels through the multi-branching and tapered structure of the arterial bed. This causes reflections to occur due to the tapering [10], mismatched bifurcations, and changes in mechanical properties [9]. This inherently generated plethora of reflected waves with varying timing and amplitude. However, tracking these waves using a single tube [40] or T-tube [45] is inadequate as they assume only one or two effective reflection sites, respectively, which may not account for the full range of reflections that occur.

The single tube and T-tube approaches aim to determine the distance to an effective reflection site away from the heart. However, their assumptions may not accurately reflect the complex nature of the arterial bed and its multiple reflection sites. Therefore, alternative methods may be required to fully capture and analyze the multitude of reflections generated by the arterial bed. The concept of effective distance to a reflection site has traditionally been determined by the quarter wavelength formula [46] but was challenged by [47].

Burattini and Di Carlo [48] proposed a modified approach to the T-tube method, where they suggested the resultant of all reflecting sites in the upper part of the body is likely to dominate over the resultant of all reflecting sites in the lower part of the body. Although they used a frequency domain approach, our findings using a time domain model are consistent with their suggestion. Using a time domain model, as applied in this study, enables the investigation of the intricate structure of the arterial tree and the tracking of local reflections as they propagate back towards the heart. This approach represents a significant advancement in the understanding of the nature, size, and timing of reflections across all simulated segments of the arterial tree.

Keeping in mind the simplifications and assumptions of this study, such as using a narrow-gaussian pulse, our results suggest that, in a healthy physiological setting, most of the reflections present in the ascending aorta originate from the carotid arteries rather than the more distal locations in lower body. While our sim-

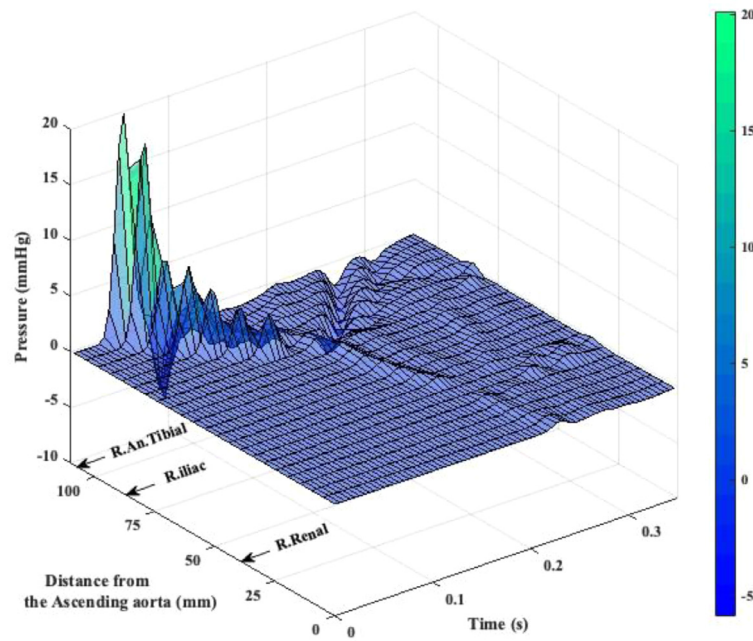


**Fig. 4.** The amplitude of the pressure pulse propagating in the arterial tree from the right anterior tibial artery (R. anterior tibial) to the aortic root. The length of the travelled arterial path is 117 cm. R. iliac: right iliac artery; R. renal: right renal artery.

**Table 2**

Comparison of the reflection coefficients when the wave encounters the major bifurcations in the forward (from the parent vessel) and backward (from one of the daughter vessels) directions.

ROUTE	MAJOR BIFURCATIONS	FORWARD	BACKWARDS
ANTERIOR TIBIAL	Aortic arch-thoracic aorta	-0.045	-0.067
	Abdominal aorta-renal arteries	0.0081	0.07
	Abdominal aorta-iliac arteries	0.052	0.55
	Iliac artery-tibial arteries	0.059	0.49
RENAL	Aortic arch-thoracic aorta	0.045	0.067
	Abdominal aorta-renal artery	0.063	0.92
	Ascending aorta-renal artery	0.29	0.43
BRACHIAL	Innominate artery-subclavian artery	0.09	0.66
	Subclavian artery-radial artery	0.038	0.49
	Ascending aorta-innominate artery	0.29	0.43
CAROTID	Innominate artery-carotid artery	0.09	0.43

ulations using different pulse durations and amplitudes showed no influence of the ratios of peak pressures in the ascending aorta, selection of a narrow Gaussian-shaped pulse as an input simplified the tracking of the backward waves.

Despite being a simplification of reality, 1D models of the circulation are useful tools to understand the function of the arterial tree [49]. The aim of this study was to examine the size of reflections resulting from waves crossing arterial bifurcations in the backward direction in a tapered 1D model. We also aimed to investigate the size of reflected waves that reach the ascending aorta that arise from various arterial locations in the upper and lower body. Although, this problem has been studied before, in the present work we revisited the question using a new approach; rather than studying wave propagation from the heart to the periphery (forward direction), we examined the propagation of waves travelling towards the heart (backward direction).

The results of our analysis provide further evidence that the reflection coefficients in physiological bifurcations are direction-dependant, with larger absolute values in the backwards direction (bifurcation approached from the daughter vessels) compared to the forward direction (bifurcation approached from the parent vessel). The finding is consistent with previous experimental observations of Papageorgiou and colleagues [6], who found that, in a healthy human arterial tree, most bifurcations are well-matched

in the forward direction. Using data from Cox and Pace [50] for the ascending aorta, brachiocephalic, left subclavian artery and descending aorta, Borlotti et al. [51] calculated the characteristic impedances for these vessels in anaesthetized dogs and found that the reflection coefficient is 0.02 in the forward direction and -0.48 in the backward direction. This shows that the reflection coefficient is highly dependent on the direction of wave encountering the bifurcation. Physiological bifurcations are well-matched (i.e., optimal area ratio) with low values of  $R$  for forward (parent to daughters), and unmatched with high values of  $R$  for a wave travelling in the opposite direction (daughter to parent and other daughter). Further, our results explain the *in-vivo* experimental observations of Peterson and Gerst [13], who observed no change in the pressure at the root of the aorta when pulses were inserted from peripheral arterial locations in living dogs. We found a similar pattern in our study, where pulses originated from renal and radial arteries lost most of their amplitude on route to the aortic root (Fig. 5). Moreover, our results showed that the backward wave originated at the right common carotid reached the ascending aorta with approximately 18% of their magnitude. This was expected, as reflected waves in the carotid encounter fewer number of bifurcations and travel a considerably shorter distance to reach the aortic root compared to backward waves originating at other more distal locations.

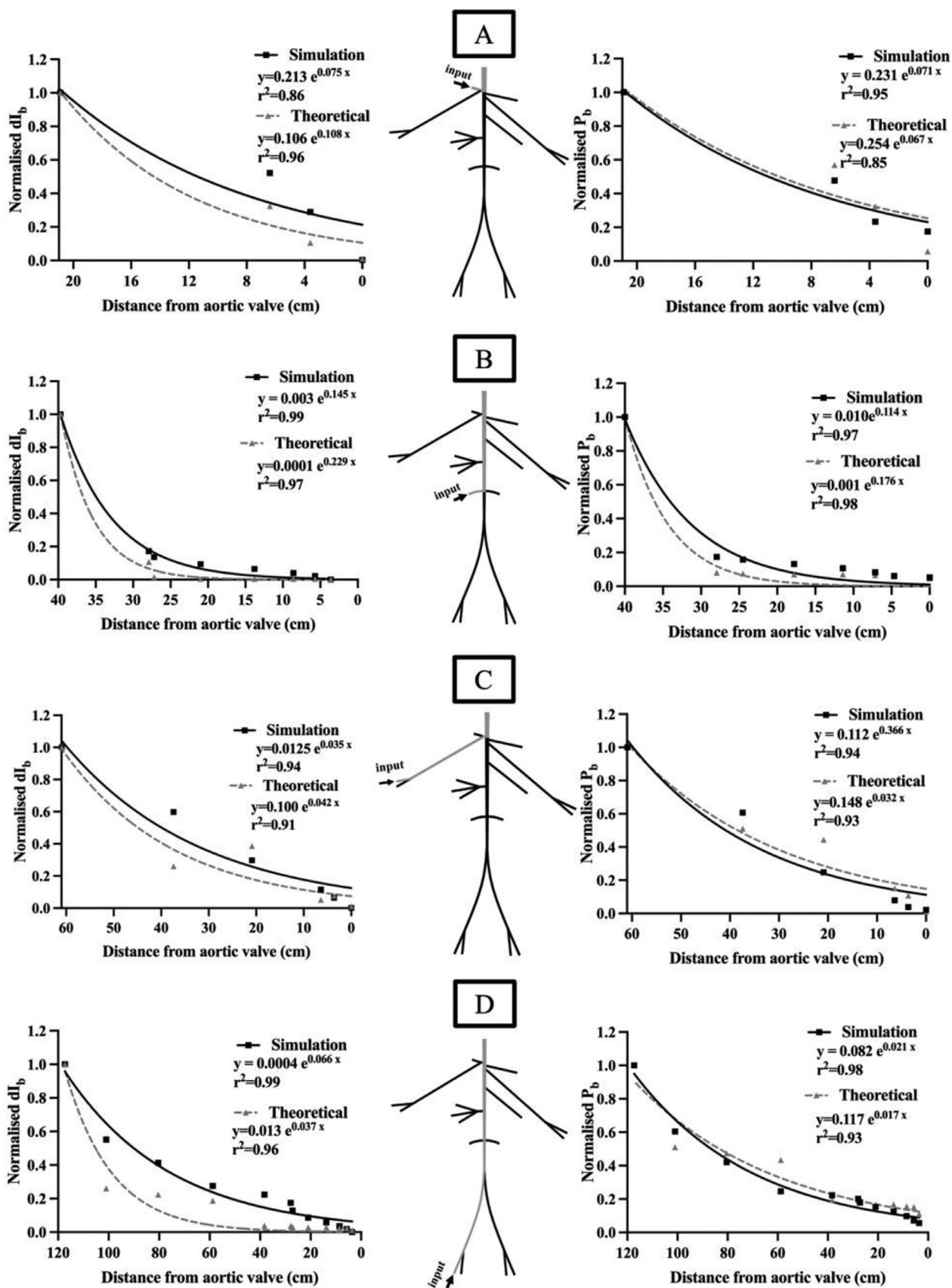


**Fig. 5.** Comparison between the theoretical (i.e., calculated using  $R_t$ ) and simulated amplitudes of transmitted pressure wave (right panels) and wave intensity (left panels). Dashed and solid lines represent an exponential fitting for the reduction of the pressure and backward wave intensity. The triangle markers represent the theoretical calculation, and the square represents the simulation results. The fitted function is provided and  $r^2$  values indicate the goodness of the fitting. The values are normalised to the amplitude of the injected pulse at the right carotid artery in A, at right radial artery in B, at the right renal artery in C, and at the right anterior tibial artery in D. Corresponding travelled distances were 20, 60, 40 and 120 cm, respectively. The scale of the x-axes is presented with the zero indicating the site of the ascending aorta.

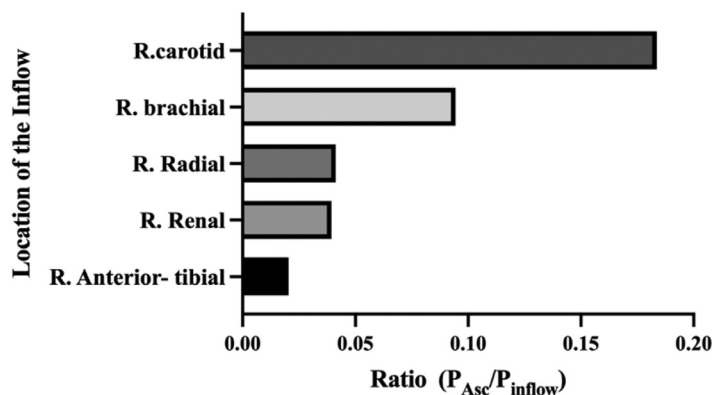


Fig. 6. The ratio of the amplitude of the pressure pulse inserted at different distal locations to that reaching the ascending aorta. Similar values were observed as we doubled and tripled the amplitude of the injected pulse.

R. carotid: Right carotid artery; R. brachial: right brachial artery; R. radial: right radial artery; R. Renal: right renal artery; R. Anterior tibial: right anterior tibial artery.

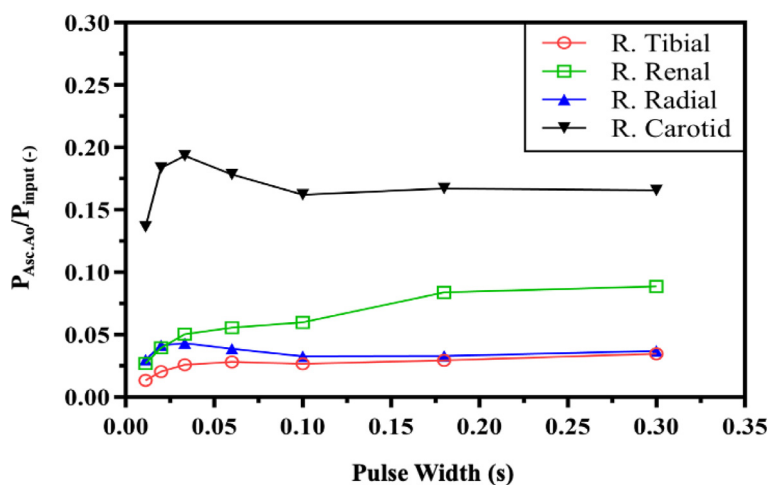


Fig. 7. Influence of pulse width on the normalised pressure arriving to the ascending aorta from different peripheral sources.

R. carotid: Right carotid artery; R. radial: right radial artery; R. Renal: right renal artery; R. Anterior tibial: right anterior tibial artery.

Similar to our study, Alastruey and colleagues [52] used 1D modeling of the systemic circulation to investigate the propagation of waves. However, their study design was different from ours, as they inserted a single pulse wave at the aortic root rather than from a distal location. Nevertheless, they found that the absolute amplitude of the wave declines exponentially, regardless of its sign. In our study, we observed the same exponential decrease of the pressure wave amplitude as it propagated backward in the arterial tree (Fig. 5). Similar findings were also reported by Hinstead and Anliker [53]. This trend was also preserved in the wave intensity ( $dI$ ) pattern, which was consistent with results reported in non-tapered in vitro model of the arterial tree [54].

Previous works have examined the differences between different methods of estimating  $R$  both numerically and experimentally. Li et al. [41] studied  $R$  experimentally *in-vitro* using multiple sets of straight flexible tubes with known mechanical properties, while Mynard and colleagues [44] studied  $R$  computationally in a single non-tapered vessel. Both studies agreed that  $R$  calculated from the separated pressure ( $R_{dp}$ ) and from the square root of the separated wave intensity ( $R_{dl}^{0.5}$ ) showed the strongest agreement with the theoretical coefficient  $R_t$ .

Consistent with the findings of Li et al. [41], our results show that  $R_{dl}^{0.5}$  underestimates values of the wave intensity compared to those determined using  $R_t$ . The reason for this underestimation maybe explained by the results in Mynard et al. [44], who showed higher error in reflection coefficients calculated by wave intensity

in nonlinear conditions. On the other hand, the transmitted pressure amplitude calculated using  $R_{dp}$  showed good agreement with that calculated with  $R_t$ . While *in-vitro* comparison of the reflection coefficient in [41] showed that  $R_{dp}$  overestimates  $R_t$ , in this study, the same trend is not observed as shown in Fig. 5 and Table 1. The difference may be due to the overlapping of the pressure waves caused by tapering and the short length of the vessels.

According to [41], the magnitude of the local reflection coefficient varies with their proximity to the reflection site. The tapering of the vessel causes multiple infinitesimal reflections [4,10], and although the size of these reflected waves is small, amalgamated collectively they might be affecting the values estimated by  $R_{dp}$  and  $R_{dl}^{0.5}$ .

This study has focused solely on the effect of pressure wave reflection in the aorta, which is a crucial factor in determining cardiac function [55]. However, it is imperative that future research investigates the influence of reflected waves and resultant pressure changes in various arterial locations, particularly those vessels that supply blood to vital organs. Such investigation would hold significant scientific importance and should be considered as an essential aspect of future studies.

Based on the current findings, the largest proportion of reflected waves observed at the ascending aorta is attributed to reflections from the upper body. This warrants clinical investigation to inform the possible management of arterial diseases that affect arterial bifurcation morphologies.

Furthermore, our approach takes into consideration the impact of tapering on reflection, which has not been extensively explored in previous studies. By incorporating tapering into our model, we are able to capture the influence of this important factor on reflection, which can have significant implications for the interpretation of clinical data. This demonstrates the importance of a comprehensive understanding of the complex mechanisms underlying arterial reflection and highlights the need for continued research in this area.

## 5. Limitations

The approach implemented in this study is to induce a narrow-gaussian pulse wave at distal arterial sites and observe the amplitude of the wave reaching the aortic root. However, there are some limitations to this approach. Firstly, to simplify the problem and focus on the reflected waves, the influence of the pumping heart on the response of the system was not considered. Nonetheless, our results are in consistent with earlier in-vivo experimental work that accounted for the beating heart [13]. A second limitation of the study was using the same value of pressure pulse amplitude at each of the distal sites, despite the possibility that reflections originating from different sites along the arterial bed may not have the same amplitude. This approach was adopted to enable a comparison of the amplitude of waves arriving to the ascending aorta. Moreover, with this approach we kept the arterial dimensions in physiological range and studied reflections arising from vessels with different cross-sectional areas. Thirdly, by using a narrow gaussian pulse, this study did not consider the effect of overlapping of reflections that occurs in high-frequency waves.

## 6. Conclusions

The physiological bifurcations considered in this work have a much larger reflection coefficient when the pulse wave encounter them in the backward than the forward direction. The implication of which is that amplitudes of waves travelling backwards are continuously reduced and the further the origin of the backward wave is the less likely for it to be discerned in the aortic root. Reflected waves detected in the ascending aorta are likely to originate at proximal arterial sites and are much larger when originated in the upper compared to lower body. Based on the current findings, the largest proportion of reflected waves observed at the ascending aorta is attributed to reflections from the upper body. This highlights the need for clinical research to inform potential management strategies for arterial diseases that impact arterial bifurcation morphologies.

## Author contributions

S.A. and A.W.K conception and design of research; S.A. prepared figures and drafted the manuscript; S.A. and A.W.K interpreted the results of simulations; S.A. and A.W.K edited, revised, and approved final version of manuscript.

## Declaration of Competing Interest

The authors declare that the research was conducted in the absence of any commercial or financial relationships that could be construed as a potential conflict of interest.

## Acknowledgments

The authors gratefully acknowledge Dr Alessandro Giudici for his valuable contribution in proofreading and providing suggestions to improve the study.

## References

- [1] P.C. Luchsinger, R.E. Snell, D.J. Patel, D.L. Fry, Instantaneous pressure distribution along the human aorta, *Circ. Res.* 15 (1964) 503–510.
- [2] M.F. O'Rourke, J.V. Blazek, C.L. Morreels, L.J. Krovetz, Pressure wave transmission along the human aorta. Changes with age and in arterial degenerative disease, *Circ. Res.* 23 (4) (1968) 567–579.
- [3] B.E. Westerhof, J.P. Van Den Wijngaard, J.P. Murgo, N. Westerhof, Location of a reflection site is elusive: consequences for the calculation of aortic pulse wave velocity, *Hypertension* 52 (3) (2008) 478–483.
- [4] J.E. Davies, J. Alastruey, D.P. Francis, N. Hadjiloiou, Z.I. Whinnett, C.H. Manisty, et al., Attenuation of wave reflection by wave entrapment creates a "Horizon Effect" in the human aorta, *Hypertension* 60 (2012) 778–785.
- [5] P. Segers, M.F. O'Rourke, K. Parker, N. Westerhof, A. Hughes, J. Aguado-Sierra, et al., Towards a consensus on the understanding and analysis of the pulse waveform: results from the 2016 workshop on arterial hemodynamics: past, present and future, *Artery Res* 18 (2017) 75–80 Jun.
- [6] G.L. Papageorgiou, B.N. Jones, V.J. Redding, N. Hudson, The area ratio of normal arterial junctions and its implications in pulse wave reflections, *Cardiovasc. Res.* 24 (1990) 478–484.
- [7] V.L. Streeter, W.F. Keitzer, D.F. Bohr, Pulsatile pressure and flow through distensible vessels, *Circ. Res.* 13 (1963) 3–20.
- [8] A.W. Khir, K.H. Parker, Measurements of wave speed and reflected waves in elastic tubes and bifurcations, *J. Biomech.* 35 (6) (2002) 775–783 Jun.
- [9] J.J. Wang, K.H. Parker, Wave propagation in a model of the arterial circulation, *J. Biomech.* 37 (4) (2004) 457–470 Apr.
- [10] S. Abdullateef, J. Mariscal-Harana, A.W. Khir, Impact of tapering of arterial vessels on blood pressure, pulse wave velocity, and wave intensity analysis using one-dimensional computational model, *Int. J. Numer. Method Biomed. Eng.* (2020) Feb;.
- [11] GCV Den Bos, N. Westerhof, G. Elzinga, P. Sipkema, Reflection in the systemic arterial system: effects of aortic and carotid occlusion, *Cardiovasc. Res.* 10 (1976) 565–573.
- [12] A.W. Khir, K.H. Parker, Wave intensity in the ascending aorta: effects of arterial occlusion, *J. Biomech.* 38 (4) (2005) 647–655 Apr.
- [13] L.H. Peterson, P.H. Gerst, Significance of reflected waves within the arterial system, *Fed. Proc.* 15 (496) (1956) 145.
- [14] K.B. Campbell, J.A. Ringo, C. Neti, J.E. Alexander, Informational analysis of left-ventricle/systemic-arterial interaction, *Ann. Biomed. Eng.* 12 (2) (1984) 209–231 Mar.
- [15] N. Westerhof, G.C. van den Bos, S. Laxminarayan, Arterial reflection, in: R. Bauer, R. Busse (Eds.), *The Arterial System*, Springer, Berlin, Heidelberg, 1978, pp. 48–62.
- [16] R. Burattini, K.B. Campbell, Modified asymmetric T-tube model to infer arterial wave reflection at the aortic root, *IEEE Trans. Biomed. Eng.* 36 (8) (1989) 805–814.
- [17] M.F. O'Rourke, Pressure and flow waves in systemic arteries and the anatomical design of the arterial system, *J. Appl. Physiol.* 23 (2) (1967) 139–149.
- [18] P. Segers, P. Verdonck, Role of tapering in aortic wave reflection: hydraulic and mathematical model study, *J. Biomech.* 33 (3) (2000) 299–306.
- [19] J.P. Murgo, N. Westerhof, J.P. Giolma, S.A. Altobelli, Aortic input impedance in normal man: relationship to pressure wave forms, *Circulation* 62 (1) (1980) 105–116.
- [20] C.J. Mills, I.T. Gabe, J.H. Gault, D.T. Mason, J. Ross, E. Braunwald, et al., Pressure-flow relationships and vascular impedance in man, *Cardiovasc. Res.* 4 (4) (1970) 405–417.
- [21] T. Murakami, Squatting: the hemodynamic change is induced by enhanced aortic wave reflection, *Am J Hypertens [Internet]* 15 (11) (2002) 986–988 Nov 1.
- [22] R.D. Latham, N. Westerhof, P. Sipkema, B.J. Rubal, P. Reuderink, J.P. Murgo, Regional wave travel and reflections along the human aorta: a study with six simultaneous micromanometric pressures, *Circulation* 72 (6) (1985) 1257–1269.
- [23] M.S. Olufsen, C.S. Peskin, W.Y. Kim, E.M. Pedersen, A. Nadim, J. Larsen, Numerical simulation and experimental validation of blood flow in arteries with structured-tree outflow conditions, *Ann. Biomed. Eng.* 28 (11) (2000) 1281–1299 Nov.
- [24] B.N. Steele, J.P. Ku, T.J.R. Hughes, C.A. Taylor, In vivo validation of a one-dimensional finite-element method for predicting blood flow in cardiovascular bypass grafts, *IEEE Trans. Biomed. Eng.* 50 (6) (2003) 649–656.
- [25] M. Willemet, V. Lacroix, E. Marchandise, Validation of a 1D patient-specific model of the arterial hemodynamics in bypassed lower-limbs: simulations against in vivo measurements, *Med. Eng. Phys.* 35 (11) (2013) 1573–1583 Nov.
- [26] P. Segers, E.R. Rietzschel, M.L. De Buyzere, S.J. Vermeersch, D. De Baquer, L.M. Van Bortel, et al., Noninvasive (input) impedance, pulse wave velocity, and wave reflection in healthy middle-aged men and women, *Hypertension* 49 (6) (2007) 1248–1255 Jun.
- [27] S.E. Greenwald, A.C. Carter, C.L. Berry, Effect of age on the in vitro reflection coefficient of the aortoiliac bifurcation in humans, *Circulation* 82 (1) (1990) 114–123.
- [28] A. Swillens, L. Lanoye, J. De Backer, N. Stergiopoulos, P.R. Verdonck, F. Vermassen, et al., Effect of an abdominal aortic aneurysm on wave reflection in the aorta, *IEEE Trans. Biomed. Eng.* 55 (5) (2008) 1602–1611 May.
- [29] T. Murakami, Enhanced aortic pressure wave reflection in patients with aortic coarctation after aortic arch repair, *Pulse* 5 (1–4) (2017) 82–87.
- [30] M.A. Quail, R. Short, B. Pandya, J.A. Steeden, A. Khushnood, A.M. Taylor, et al., Abnormal wave reflections and left ventricular hypertrophy late after coarctation of the aorta repair, *Hypertension* 69 (3) (2017) 501–509.

- [31] N. Stergiopoulos, M. Spiridon, F. Pythoud, J.J. Meister, On the wave transmission and reflection properties of stenoses, *J. Biomech.* 29 (1) (1996) 31–38.
- [32] K.S. Matthys, J. Alastruey, J. Peiró, A.W. Khir, P. Segers, P.R. Verdonck, et al., Pulse wave propagation in a model human arterial network: assessment of 1-D numerical simulations against in vitro measurements, *J. Biomech.* 40 (15) (2007) 3476–3486.
- [33] J. Alastruey, K.H. Parker, S.J. Sherwin, Arterial pulse wave haemodynamics, in: BHR Group - 11th International Conferences on Pressure Surges, 2012, pp. 401–442.
- [34] A. Giudici, Y. Li, Cleary S Yasmin, K. Connolly, C. McEniery, et al., Time-course of the human thoracic aorta ageing process assessed using uniaxial mechanical testing and constitutive modelling, *J. Mech. Behav. Biomed. Mater.* (2022 Oct 1) 134.
- [35] P.B. Dobrin, Mechanical properties of arteries, *Physiol. Rev.* 58 (2) (1978) 397–460.
- [36] A.I. Moens, *Over De Voortplantingssnelheid Ven Den Pols*, 1877 Leiden, The Netherlands.
- [37] N. Stergiopoulos, Y. Tardy, J.J. Meister, Nonlinear separation of forward and backward running waves in elastic conduits, *J. Biomech.* 26 (2) (1993) 201–209 Feb.
- [38] F. Pythoud, N. Stergiopoulos, J.J. Meister, Separation of arterial pressure waves into their forward and backward running components, *J. Biomech. Eng.* 118 (3) (1996) 295–301 Aug.
- [39] J.P. Mynard, M.R. Davidson, D.J. Penny, J.J. Smolich, Non-linear separation of pressure, velocity and wave intensity into forward and backward components, *Med. Biol. Eng. Comput.* 50 (6) (2012) 641–648 Jun.
- [40] M.J. Lighthill, Waves in fluids, *Commun. Pure Appl. Math.* 20 (2) (1967) 267–293.
- [41] Y. Li, K.H. Parker, A.W. Khir, Using wave intensity analysis to determine local reflection coefficient in flexible tubes, *J. Biomech.* 49 (13) (2016) 2709–2717 Sep.
- [42] N. Westerhof, P. Sipkema, Bos GCV Den, G Elzinga, Forward and backward waves in the arterial system, *Cardiovasc. Res.* 6 (6) (1972) 648–656 Nov.
- [43] K.H. Parker, C.J.H. Jones, Forward and backward running waves in the arteries: analysis using the method of characteristics, *J. Biomech. Eng.* 112 (3) (1990) 322–326 Aug.
- [44] J. Mynard, D.J. Penny, J.J. Smolich, Wave intensity amplification and attenuation in non-linear flow: implications for the calculation of local reflection coefficients, *J. Biomech.* 41 (16) (2008) 3314–3321 Dec.
- [45] O'Rourke M.F., Avolio A.P. Pulsatile flow and pressure in human systemic arteries. Studies in man and in a multibranched model of the human systemic arterial tree. *Circ. Res.* 46(3):363–72.
- [46] M.F. O'Rourke, Vascular impedance — a call for standardisation, in: *Cardiovascular System Dynamics*, Springer, Boston, MA, 1982, pp. 175–179.
- [47] P. Sipkema, N. Westerhof, Effective length of the arterial system, *Ann. Biomed. Eng.* 3 (3) (1975) 296–307.
- [48] R. Burattini, S. Di Carlo, Effective length of the arterial circulation determined in the dog by aid of a model of the systemic input impedance, *IEEE Trans. Biomed. Eng.* 35 (1) (1988) 53–61.
- [49] N. Westerhof, G. Elzinga, P. Sipkema, An artificial arterial system for pumping hearts, *J. Appl. Physiol.* 31 (5) (1971) 776–781 Nov.
- [50] Cox R.H., Pace J.B. Pressure-flow relations in the vessels of the canine aortic arch. *1975;228(1):1–10.*
- [51] A. Borlotti, C. Park, K.H. Parker, A.W. Khir, Reservoir and reservoir-less pressure effects on arterial waves in the canine aorta, *J. Hypertens.* 33 (3) (2015) 564–574 Mar 6.
- [52] J. Alastruey, K.H. Parker, J. Peiró, S.J. Sherwin, Analysing the pattern of pulse waves in arterial networks: a time-domain study, *J. Eng. Math.* 64 (4) (2009) 331–351.
- [53] M.B. Hstand, M. Anliker, Influence of flow and pressure on wave propagation in the canine aorta, *Circ. Res.* 32 (4) (1973) 524–529.
- [54] J. Feng, Q. Long, A.W. Khir, Wave dissipation in flexible tubes in the time domain: in vitro model of arterial waves, *J. Biomech.* 40 (10) (2007) 2130–2138.
- [55] C.M. Park, A.D. Hughes, M.Y. Henein, A.W. Khir, Mechanisms of aortic flow deceleration and the effect of wave reflection on left ventricular function, *Front. Physiol.* 11 (November) (2020) 1–10.